KINETICS OF THE NITROUS OXIDE - HYDROGEN REACTION

Hans Henrici, Margaret Hunt, and S. H Bauer

Department of Chemistry, Cornell University
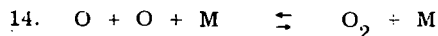
Ithaca, New York 14850

The reaction between nitrous oxide and hydrogen was investigated over the temperature range 1700°-3000^OK in shock heated mixtures, diluted 1%-3% (for each reagent) in argon. Incident shock densities were (1-7) 10^{-6} moles cm^{-3}. Most of the rate data were obtained by recording the absorption of characteristic OH radiation at 3094Å; additional spectrophotometric measurements were made at 2259Å (for NO) and at 2300 Å (for N_2O). The first objective was to determine whether the literature values for the rate constants of the elementary steps adequately account for the observed OH profiles, and the second, to deduce more reliable values for those constants the magnitudes of which are in doubt. Preliminary analysis of the data indicated that the OH concentration exceeded its equilibrium level particularly at the lower temperatures; this was also the case for NO. Detailed analyses using a shock kinetics program for 14 reactions (and their inverses) show that the "best" values generally accepted for the various rate constants lead to much faster rise times but lower maximum concentrations of OH than were observed. In view of the consensus currently being reached regarding the constants for the O/H reactions, our data place lower limits on the magnitudes for the (N_2O + O) steps and an upper limit for the (N_2O + H) step.

STATEMENT OF THE PROBLEM

The reaction between nitrous oxide and hydrogen at high temperatures is very rapid. While the main outlines of the mechanism may be formulated with reasonable certainty, the magnitudes of the kinetics parameters are not well established. In particular, several of the critical rate constants have been measured at lower temperatures only, and information which permits extrapolation to the higher temperature regime (up to 3000^OK) is not available. The entire sequence of steps may be divided into three groups.

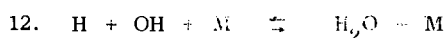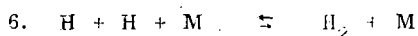I. The following involve oxygen and nitrogen only;

the initiation reaction

$$1. \quad N_2O + M \quad \rightarrow \quad N_2 + O + M$$

the depletion reactions

$$2. \quad N_2O + O \quad \rightarrow \quad N_2 + O_2$$

$$3. \quad N_2O + O \quad \rightleftharpoons \quad 2 NO$$

scrambling and recombination steps

$$7. \quad O + NO \quad \rightleftharpoons \quad O_2 + N$$

$$8. \quad O + N_2 \quad \rightleftharpoons \quad NO + N$$

$$14. \quad O + O + M \quad \rightleftharpoons \quad O_2 + M$$

II. This group involves oxygen and hydrogen only; all but the termolecular reactions are very rapid.

the primary step

    4. $O + H_2 \rightleftharpoons OH + H$

secondary steps

    9. $O + OH \rightleftharpoons O_2 + H$

    10. $OH + H_2 \rightleftharpoons H_2O + H$

    11. $OH + OH \rightleftharpoons H_2O + O$

    13. $OH + OH \rightleftharpoons H_2 + O_2$

    6. $H + H + M \rightleftharpoons H_2 + M$

    12. $H + OH + M \rightleftharpoons H_2O + M$

III Reactions which couple the N/O to the H/O system;

the primary step

    5. $H + N_2O \rightarrow N_2 + OH$

secondary steps (of little consequence under shock conditions)

    16. $NO + H_2 \rightleftharpoons HNO + H$

    17. $NO + H_2O \rightleftharpoons HNO + OH$

    15. $HNO + M \rightleftharpoons H + NO + M$

    18. $N_2O + OH \rightleftharpoons HNO + NO$

The reactions for which the rate constants are best established are the initiation step and some of the reactions in group (II). The rate constant for reaction (1) has been measured[1] over four powers of ten between 1500° and 2500^OK. These experiments were conducted at a total density starting at 5×10^{-6} moles/cm^3 and into the high pressure saturation region. The rate of N_2O decomposition was found to be proportional to the density up to 6×10^{-5} moles/cm^3, a level which is much higher than the highest densities in our experiments. In group (II), the best known rate constants are those for reaction (9), which was determined to within 10% over the temperature range 1300° to 1700^OK, and for reaction (4) which was determined in the same study combined with literature values available at lower temperatures. Reaction (5), the primary coupling step between groups (I) and (II) is the least well established of the controlling steps in the overall process. The thermochemical parameters for the above reactions are known with considerable precision, except possibly those involving HNO. The relevant data used in the following calculations were taken from the JANAF Tables.

The reaction rates between nitrous oxide and hydrogen were measured in shock heated mixtures (incident regime) over the temperature range 1700°-$3000^{\circ}K$. The first objective was to determine whether the literature values for the rate constants of the elementary steps do adequately account for such data; the second, to deduce more reliable values for those constants the magnitudes of which are in doubt. The $(N_2O + H_2)$ reaction is typical of complex oxidation systems and is particularly well suited for a shock tube study. Several spectroscopic probes are available as "handles" on the course of the reaction. Most of the data collected during this investigation were obtained by recording the absorption of characteristic OH radiation; additional spectro-photometric measurements were made in absorption for NO and for N_2O. When both of these gases were present, the net absorption at $2259\overset{\circ}{A}$ was corrected for that due to N_2O. Other probes which are available for following this reaction are the intensities of emission in the infrared due to OH, H_2O and NO; these were not used in the present study. The mixtures of N_2O/H_2 used were, 1/1, 1/2, 1/3, 3/1, 3/3% in argon, with total densities from $(1-7)\ 10^{-6}$ moles cm^{-3}. The levels of OH generated ranged 1.2×10^{-8} to 2.3×10^{-9} moles cm^{-3}.

EXPERIMENTAL PROGRAM

All our data were obtained in the incident shock regime, using a 6" I.D. stainless steel shock tube. It has an 8' driver section and a 30' test section. The observation windows are 26' downstream from the diaphragm. Prior to filling, the experimental section was pumped down to 10^{-4} torr; the apparent leak rate was 2.5×10^{-6} torr/min. Mylar diaphragms of 0.008" thickness were cross-cut to 0.005" and pressure broken. The speed of the incident shock wave was measured with a raster system, upon which calibrated markers were superposed at $10\mu sec$. intervals. The raster was triggered by a piezoelectric pressure transducer. Further downstream were three platinum heat gauges with known separation. The error in the shock speed was estimated to be about 0.1%. The peizoelectric gauge also triggered the other electronic devices, including the discharge through the H_2O vapor lamp. We estimated the time constant of the recording system to be about $5\mu sec$.

The N_2O used in these studies was doubly distilled in vacuum, mixed with hydrogen and argon in large glass vessels or in glass lined metal tanks and kept at least 10 hours before using, to insure complete mixing. Mass spectrometric checks revealed no oxygen impurity above the background level of the spectrometer.

The source of characteristic OH radiation was described previously[15]. The lamp emission was made parallel before entering the shock tube, and the exit light was focused onto the entrance slit of a Jarrell-Ash 500 mm focal length monochromator (JACO 8200), which has a $16\overset{\circ}{A}/mm$ dispersion. In order to discriminate against the emission from the shock heated gas, the focusing lens was placed 70 cm from the exit window of the shock tube. Forty micron entrance and exit slits permitted selection of a portion $(\Delta\lambda = 0.64\overset{\circ}{A})$ of the Q branch head $(3094\overset{\circ}{A})$ of the $^2\Sigma^+ - ^2\Pi$ transition. The time rate of change in the concentration of N_2O and the final concentration of NO were measured using a deuterium arc*, as a source of continuum radiation.

For the NO absorption measurements, a wavelength region around $2259\overset{\circ}{A}$ $(\pm 2.7\overset{\circ}{A})$ was selected, this belongs to the γ band (0, 0 of $^2\Sigma^+ - ^2\Pi_{3/2, 1/2}$) transition. The average of 8 runs with 1% NO in argon, the absorption coefficient between 1800° and $2100^{\circ}K$ was determined to be 8.55 $(\pm 0.3) \times 10^{+4}\ cm^2/mole$. For these measurements the NO was obtained from a commercial cylinder, and doubly distilled to remove N_2

---

* WHS 200 lamp, Dr. Kern, Göttingen.

and the higher oxides of nitrogen. Since N_2O absorbs only at shock temperatures, a reliable determination of the NO concentration in the reacting mixture was possible only after the N_2O had decomposed. The absorption of the generated NO remained constant for at least 1 msec, laboratory time, when the gas consisted initially of a mixture of pure N_2O in Ar, and also when hydrogen was added. The absorption coefficient of N_2O at 2300Å as a function of temperature, has been determined by Troe[16]. The few preliminary measurements made in our laboratory do not disagree with that determination.

Test times ranged up to 500μsec; however, most of the runs were taken up to 350μsec only. Particle times were therefore of the order of 1500μsec.

TYPICAL RESULTS AND PRELIMINARY ANALYSIS

Within the limits of the time constants of these measurements the OH concentration rises linearly with a finite slope for a period of 50 to 100μsec, then slowly bends over and appears to approach a level value. In some cases there were clear indications that this passed through a maximum. The preliminary assumption that the maximum level of OH corresponded to the equilibrium concentration proved misleading. An equilibrium shock program not only gave values for the final reaction temperature (which ranged from $100-250°$ above shock temperatures calculated for no reaction) but also gave the equilibrium concentration of all the species. Comparison of the calculated with the observed values, based on the approximate absorption coefficient (for OH) of 2.2×10^6 cm^2/mole is shown in Table I. It is clear that the overshoot is higher at the lower temperature. The cause for the overshoot is the same as in the H/O system, in that three body processes which reduce the atom and free radical concentrations are slow compared to the steps which produce OH, or bring it into local equilibrium with the other radicals. These preliminary studies also showed that the simplifying assumption regarding the OH production [i.e. that it is primarily controlled by reactions (1), (2), (3), and (4)] does not account for the data. Under the steady-state assumption for the oxygen atoms,

$$\frac{d(OH)}{dt} = k_1 [N_2O] [M] \left[1 + \frac{k_3 + k_4}{k_2} \frac{[N_2O]}{[H_2]} \right]^{-1} \qquad ; \text{ see Fig. 1 .}$$

A test of this equation can be made by assuming literature values for $k_2^{(1A)}$, $k_3^{(2)}$, and $k_4^{(3)}$. This reduction is not acceptable in view of the fact that runs with different concentrations of N_2O and H_2 do not lie on the same line, nor does the dissociation rate constant for N_2O agree with the currently accepted value[1]. However, the various curves are close to one another and fall below the previous data on the N_2O decomposition[1A].

Not only does the OH concentration overshoot but the NO appears to behave likewise; this has been observed previously in studies of the N_2O decomposition[1A]. The proof requires measurement of the limiting value of the NO concentration, referred to the initial concentration of N_2O, which disappears completely by the time the test period is over. The ratio (in the absence of H_2),

$$\beta \equiv \frac{(NO)^\infty}{(N_2O)^i} = \frac{1}{1 + (a + b)} \approx 0.47; \; (a + b) \approx 1.1$$

where a measures the fraction of oxygen atoms used in reaction (2), and b is the fraction of oxygen atom which follow reaction (14), compared with reaction (3) as a reference. Table II is a summary of magnitudes of β for several typical runs. The sum $(a + b) = 1.1$ indicates approximately comparable depletion of oxygen atoms by reactions (2), (3), and (4). In contrast, when hydrogen is present the observed value for β is

considerably less, also shown in Table II. The values for β in absence of hydrogen check with those obtained by Gutman[1A], who reported $\beta = 0.56$ at $2515^{\circ}K$, with no detectable temperature dependence. Thus, in the presence of hydrogen a considerable fraction of the oxygen atoms are removed by the primary reaction (4), and the secondary step (9). The partition of oxygen atoms among the various reactions, in the presence of hydrogen, cannot be directly estimated from the measured β, but this does provide an additional boundary condition on the correct assignment of reaction rate constants. One may now list the available experimental parameters:

(a) the initial slope of the OH curve (absence of an induction period)
(b) the time required for the OH concentration to reach 63% of its final value
(c) the magnitude of the OH at the maximum
(d) the value of β
(e) the time required for the disappearance of N_2O to 1/2 of its initial value.

The matching of the OH concentration-time profile, and the parameters listed above were used to test combinations of rate constants, as described in the next section.

EXTENDED CALCULATIONS AND CURRENT STATUS OF THE PROBLEM

Because of the coupling of a large number of reactions and their approximately comparable contributions, no simplifying assumptions permit an analytic solution of the coupled set of differential equations. Therefore a general kinetics program was introduced to obtain calculated values for the concentration profiles of all species. The program which was obtained from Cornell Aeronautical Laboratory[18], permits the insertion of the enthalpy and free energy for each specie as a function of temperature. The thermodynamic functions are expressed as polynomials in the temperature. For the rate constants specific values must be inserted for the pre-exponential factor, the pre-exponential temperature dependence and the activation energy. This incident shock program computes the equilibrium constant for each reaction, obtains the rate constant for its reverse and gives the net rate of formation (Q_{ij}) for each species (j) from every reaction (i). It also gives the concentration of each species as a function of time and computes the temperature profile behind the shock. The printout of the Q_{ij}'s as a function of time is probably the most useful part of the output. It provides a measure of how dependent the net concentration profile for any species is on the contribution from each reaction. It helps to gauge how effectively coupled the system is, and whether some reactions which were introduced can be discarded because of their minor contributions. For example, this was found to be the case for OH derived from reactions (15, 16, 17 and 18).

In the tests which will be described below no change was made in the value for the dissociation rate constant for step (1). The study from which we took the rate constant[1] covered a wide range of total pressures and of temperatures for low concentrations of N_2O in Ar. The reported values show very little scatter from an Arrhenius line. In addition the same results were obtained behind incident and reflected shock waves, and they were crosschecked by experiments with an adiabatic piston[19]. Nevertheless, in our system, there still may be some uncertainty about the rate constant for this reaction due to the unknown collision efficiencies for activation by the species produced in the N_2O/H_2 reaction. These may be much larger than that for argon. The other rate constants were obtained from a survey of the literature and from discussions with several workers in the field; they are listed in Table III.

In a first group of tests the rate constants for reactions (2) and (3) were accepted, and only those of the H_2/O_2 system and that of reaction (5) were varied in an attempt to obtain a fit to the experimental OH profile at $2000^{\circ}K$. These tests showed that the computed rate of OH-formation, which was much faster than the observed, could be fitted only by

reducing the rate constants of reactions (5) and (10) by a factor of 30 to 40. In order to achieve a better fit for experiments at different concentrations, it was also necessary to reduce the rate constants for (9) by a factor of 10, and for (4) by 1/2. This is clearly an unacceptable combination. Figure 2a shows the contributions of the five critical reactions to the OH concentration profile (Q_{ij}) for a typical run with 1% of N_2O and 1% H_2 in Argon; Fig. 2b shows the net OH profiles, calculated and observed as well as the calculated adiabatic temperature.

In view of the consensus now being reached as to the magnitudes of the rate constants for group II, the second exploration involved the rate constants for the depletion reaction (2) and (3), and the primary coupling reaction (5). At this stage it was demonstrated that reactions (15) to (18) have no discernable effect on the OH profile. Table IV is a summary of the various combinations tested, and Figures 3a and 3b show the Q_{ij} and the net OH profile for one of the more successful combinations found to date.

As in the first series of tests for specified k_2 and k_3, the OH profile depends most sensitively on the rates of reactions (5) and (10). A difficulty in all these attempts to fit the experimental data was that the computed OH profiles yielded maximum values for the OH concentrations which were at most half as large as those observed. Whether this is due to an uncertainty in the absorption coefficient of OH or to an incorrect combination of the rate constants will be tested in calibration measurements designed to determine the absolute OH concentrations under these conditions.

If the present set of rate constants is a reasonable approximation, the effect of the different reactions on each other and on the OH profile can be described as follows. The reaction is initiated by (1) which is rapidly followed by either (2) and (3) or by (4). If NO plays no further role, the only way in which reactions (2) and (3) contribute toward the building up of OH is through (9), the reaction of the O_2 generated in reaction (2) with hydrogen atoms. Between 1100° and $1700^{\circ}K$[3] k_9 is by now known to within $\pm 10\%$. If the extrapolation to $2000^{\circ}K$ is correct, reaction (9) makes only a minor contribution to the OH generation, at least when there is no large excess of N_2O over H_2.

Apart from the current experiments there is other evidence for the stability of NO under conditions similar to those of the shock tube investigation. The decomposition of NO is a slow process as is also its rate of reaction with molecular hydrogen, reaction (16). The rate of production of HNO would have to be at least a 100 times faster than that determined by Bulewicz and Sugden[13], in order to contribute measurably. Further, the decay of pure N_2O in argon is at least 100 times faster than the loss of N_2O through[22];

$$N_2O + NO \rightarrow NO_2 + N_2 \tag{19}$$

The absorption by NO_2 at its band maximum (4200 $\overset{o}{A}$) was not detectable in the Göttingen studies on the N_2O decomposition.

It follows that, apart from the contribution of reaction (9), oxygen atoms which react with N_2O via reactions (2) and (3) are lost for the production of OH. The net rate of OH production is therefore sensitive to the ratio: $k_4/(k_2 + k_3)$. The above preliminary experiments of the magnitude for β indicate that an increase in the rates of k_2 and k_3 is required to account for the observed ratio of $[NO]^{\infty}/[N_2O]^1$. Once the ratio $k_4/(k_2 + k_3)$ is fixed, the concentration profile of OH depends strongly on the coupled reactions (5) and (10). At the beginning, when little water is present, reaction (10) is faster than reaction (5), resulting in a net consumption of OH. As reaction (10) approaches local equilibrium, reaction (5) takes over until the N_2O is consumed. By

then, the buildup of OH is completed, and OH decays slowly _via_ three body processes.

This relatively simple picture is complicated by the fact that reactions (9) and (11) also contribute to the OH profile but by an amount which is smaller than the contributions from reactions (4), (5), and (10). However, the significance of (9), (11) can be established only after the rate constants for (2), (3), and (5) have been measured. In order to achieve this, the experiments to determine β as a function of the H_2 concentration, and the profile for N_2O disappearance will be continued.

ACKNOWLEDGEMENTS

REFERENCES

1. H. A. Olschewski, J. Troe, and H. Gg. Wagner, Ber. Bunsenges. physik. Chem. 70, 450 (1966).

1A. D. Gutman, R. L. Belford, A. J. Hay, and R. Pancirow, J. Phys.Chem., 70, 1793 (1966).

2. C. P. Fenimore, and G. W. Jones, 8th (International) Symposium on Combustion, Williams and Wilkins, Baltimore 1962, p.127.

3. D. Gutman, and G. L. Schott, in print.

4. C. P. Fenimore, "Chemistry in Premixed Flames", International Encyclopedia of Physical Chemistry and Chemical Physics, Topic 19, Vol. 5, MacMillan, New York, 1964.

5. A. L. Myerson, W. S. Watt, and P. J. Joseph, in print.

6. K. L. Wray, and J. D. Teare, J. Chem. Phys., 36, 2582 (1962).

7. H. G. Glick, J. J. Klein, and W. Squire, J. Chem. Phys., 27, 850 (1957).

8. D. L. Ripley and W. C. Gardiner, Jr., J. Chem. Phys., 44, 2285 (1966).

9. W. E. Kaskan and W. G. Browne, "Kinetics of the $H_2/CO/CO_2$ System", General Electric Reentry Systems Dept., Document 635D848 (1964).

10. H. A. Olschewski, J. Troe, and H. Gg. Wagner, Z. physik. Chem., NF, 47, 383 (1965).

11. G. L. Schott, private communication.

12. K. L. Wray, 10th (International) Symposium on Combustion, The Combustion Institute, Pittsburgh, Pa., 1965, p.523.

13. E. M. Bulewicz and T. M. Sugden, Proc. Roy. Soc. (London), A277, 143 (1964).

14. K. A. Wilde, Report No. S-121, Rohm and Haas Company, Redstone Research Laboratories, Huntsville, Alabama 35807.

15. S. H. Bauer, G. L. Schott and R. E. Duff, J. Chem. Phys., 28, 1089 (1958).

16. J. Troe, Dissertation, Gottingen, 1965.

17. C.A.L. Equilibrium Normal Shock Program, Cornell Aeronautical Laboratory, Inc., Buffalo, New York 14221, September 1966.

18. L. J. Garr, P. V. Marrone, W. W. Joss, and M. Williams, Inviscid Non-equilibrium Flow Behind Bow and Normal Shock Waves, Cornell Aeronautical Laboratory, Inc., Buffalo, New York 14221,
CAL - Report No. QM - 1626 - A - 12 (I), May 1963
QM - 1626 - A - 12 (II), May 1963
and revised QM - 1626 - A - 12 (III), October 1966.

19. A. Martinengo, J. Troe, and H. Gg. Wagner, Z. physik. Chem., NF, 51, 104 (1966).

20. E. Freedman and J. W. Daibler, J. Chem. Phys., 34, 1271 (1961).

21. K. L. Wray and J. D. Teare, J. Chem. Phys., 36, 2582 (1962).

22. F. Kaufman, and J. R. Kelso, J. Chem. Phys., 23, 602 (1955).

TABLE I

$N_2O:H_2:Ar/3:3:94$

Run No.	p_o(total) torr.	$p_o \times 10^{-4}$ dynes/cm^2	U_{shock} mm/μs	T_2 ^{o}K equilibrium	obs. (OH) $\times 10^9$ plateau	calc. (OH) $\times 10^8$ equil.	(OH) obs. / (OH) eq.
82	43.2	5.7595	1.332	2078	9.965	0.194	5.12
83	37.7	5.0262	1.403	2235	12.224	0.398	3.08
79	16.5	2.2000	1.478	2386	10.292	0.438	2.35
85	13.2	1.7599	1.568	2551	9.179	0.695	1.32

$N_2O:H_2:Ar/3:1:96$

Run No.	p_o(total) torr.	$p_o \times 10^{-4}$ dynes/cm^2	U_{shock} mm/μs	T_2 ^{o}K equilibrium	obs. (OH) $\times 10^9$ plateau	calc. (OH) $\times 10^8$ equil.	(OH) obs. / (OH) eq.
64	27.0	3.5997	1.397	2110	8.424	0.244	3.45
54	21.0	2.7998	1.445	2222	9.900	0.317	3.12
92	12.5	1.6665	1.521	2394	7.642	0.384	1.99
93	10.3	1.3732	1.610	2586	7.620	0.540	1.41

$N_2O:H_2:Ar/1:1:98$

Run No.	p_o(total) torr.	$p_o \times 10^{-4}$ dynes/cm^2	U_{shock} mm/μs	T_2 ^{o}K equilibrium	obs. (OH) $\times 10^9$ plateau	calc. (OH) $\times 10^8$ equil.	(OH) obs. / (OH) eq.
31	27.0	3.3331	1.385	2064	5.558	0.0674	8.25
73	21.2	2.8261	1.446	2209	5.167	0.126	4.09
17	14.7	1.9598	1.515	2372	6.036	0.1939	3.12
16	13.3	1.7732	1.568	2494	5.905	0.249	2.37

$N_2O:H_2:Ar/1:3:96$

Run No.	p_o(total) torr.	$p_o \times 10^{-4}$ dynes/cm^2	U_{shock} mm/μs	T_2 ^{o}K equilibrium	obs. (OH) $\times 10^9$ plateau	calc. (OH) $\times 10^8$ equil.	(OH) obs. / (OH) eq.
48	13.0	1.733	1.548	2405	2.848	.0744	3.83
47	13.1	1.747	1.610	2554	2.310	.158	1.29

TABLE II

Determination of $\beta \equiv \dfrac{[NO]^{\infty}}{[N_2O]^i}$ in mixtures of N_2O: $Ar = 2:98$, and $N_2O:H_2:Ar = 2:1:98$

Total density: $(0.8 - 1.1 \times 10^{-5}$ moles/cm^3

No.	T ($^\circ$K)	β	
1	2009	0.42	
3	2085	0.48	$N_2O:Ar = 2:98$
4	2100	0.50	
5	2212	0.48	
17	1910	0.064	
18	1590	0.083	$N_2O:H_2:Ar = 2:1:97$
19	1965	0.063	
20	1995	0.072	

TABLE IV

Factors by which rate constants of Table III were varied in the second group of tests.

No.	Reaction	Test 1	Test 2	Test 3	Test 4	Test 5	Test 6	Test 7
2	$O + N_2O \rightleftarrows H_2 + O_2$	10	10	10	10	10	30	30
3	$O + N_2O \rightleftarrows 2 NO$	10	10	10	10	10	30	30
4	$O + H_2 \rightleftarrows OH + H$	1	1	1	1	1/2	1	1
5	$H + N_2O \rightleftarrows N_2 + OH$	1	1/3	1/3	1/10	1/10	1/3	1/10
10	$OH + H_2 \rightleftarrows H_2O + H$	1	1	2	1	1	1	1

TABLE III: "Best" literature values for k_i

No.	Reaction	ΔH^o_{2000} kcal/mole	ΔS^o_{2000} cal/mole deg.	K_{p2000} (atm)	$k_f \left\{ \dfrac{\text{moles}}{\text{cm}^3\text{-sec}} \right\}$	Ref.
1	$N_2O + M \rightleftharpoons N_2 + O + M$	39.87	32.59	5.85×10^2	$10^{14.7} e^{-58/RT}$	1
2	$O + N_2O \rightleftharpoons N_2 + O_2$	-82.18	0.65	1.32×10^9	$10^{13.93} e^{-28.0/RT}$	1A
3	$O + N_2O \rightleftharpoons 2 NO$	-38.92	6.73	5.29×10^5	$10^{14} e^{-28.0/RT}$	2
4	$O + H_2 \rightleftharpoons OH + H$	2.09	1.66	1.36×10^0	$10^{13.51} e^{-10.0/RT}$	3
5	$H + N_2O \rightleftharpoons N_2 + OH$	-66.50	5.56	3.02×10^8	$10^{14.48} e^{-16/RT}$	4
6	$H_2 + M \rightleftharpoons 2 H + M$	108.46	28.69	2.63×10^{-6}	$1.18 \times 10^{12} T^{\frac{1}{2}} e^{-94.5/RT}$	5
7	$O + NO \rightleftharpoons O_2 + N$	32.07	-3.05	6.77×10^{-5}	$10^{9.5} T e^{-39.1/RT}$	6
8	$N + NO \rightleftharpoons N_2 + O$	-75.32	-3.03	3.69×10^7	$10^{13.18}$	7
9	$H + O_2 \rightleftharpoons OH + O$	15.67	4.91	2.28×10^{-1}	$10^{13.89} e^{-14.45/RT}$	3
10	$OH + H_2 \rightleftharpoons H_2O + H$	-14.80	-2.81	1.01×10^1	$10^{13.6} e^{-5.7/RT}$	8
11	$2 OH \rightleftharpoons H_2O + O$	-16.89	-4.47	7.38×10^0	$10^{12.88} e^{-1/RT}$	9
12	$H_2O + M \rightleftharpoons H + OH + M$	126.26	31.51	2.61×10^{-7}	$10^{15.3} e^{-109/RT}$	10
13	$H_2 + O_2 \rightleftharpoons 2 OH$	17.76	6.57	3.16×10^{-1}	$10^{12.4} e^{-39/RT}$	11
14	$O_2 + M \rightleftharpoons 2 O + M$	122.04	31.94	4.40×10^{-7}	$10^{16.41} T^{-\frac{1}{2}} e^{-118/RT}$	12
15	$H + NO + M \rightleftharpoons HNO + M$	-52.71	-29.11	3.99×10^0	$10^{18.99} T^{-1}$ (b)	13
16	$H_2 + NO \rightleftharpoons HNO + H$	55.75	-0.41	6.60×10^{-7}	$10^{14.48} e^{-57.9/RT}$	13(a)
17	$OH + HNO \rightleftharpoons H_2O + NO$	-70.55	-2.40	1.53×10^7	$10^{13.95}$	13
18	$NO + HNO \rightleftharpoons N_2O + OH$	-14.73	-4.65	3.92×10^0	$10^{12.79} e^{-34.1/RT}$	14

a. Calculated from reverse rate constants through K_{eq}.

b. Units are mole^{-2} cm^6 sec^{-1}.
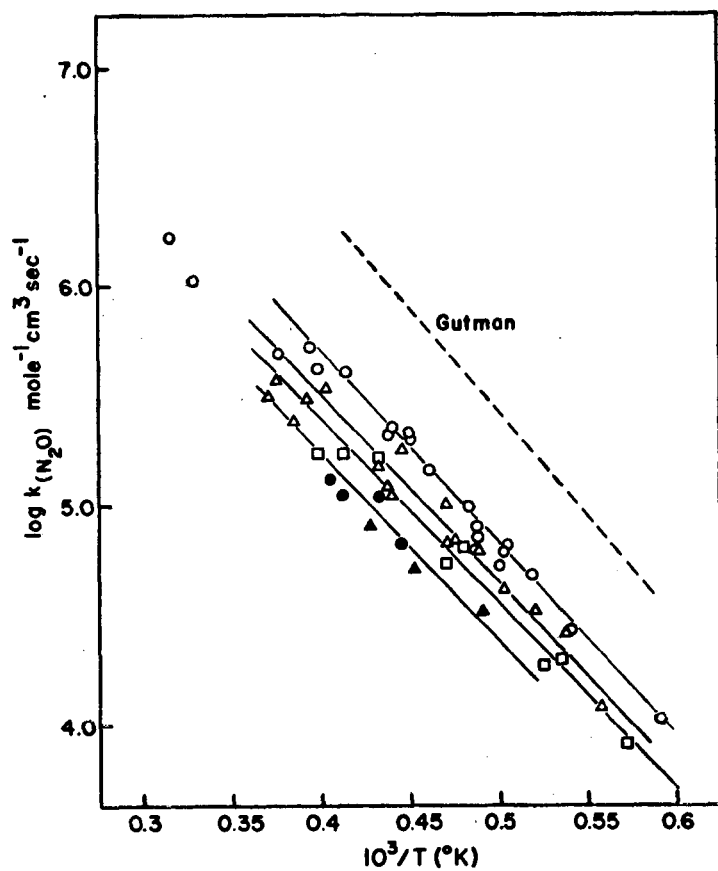
Figure 1. Bimolecular dissociation rate constant for N_2O, deduced from preliminary reduction of initial [OH] slopes.
$[N_2O]_o/[H_2]_o$ = 1:1 O; 3:1 △; 3:3 □; 1:3 ● and 2:4 ■
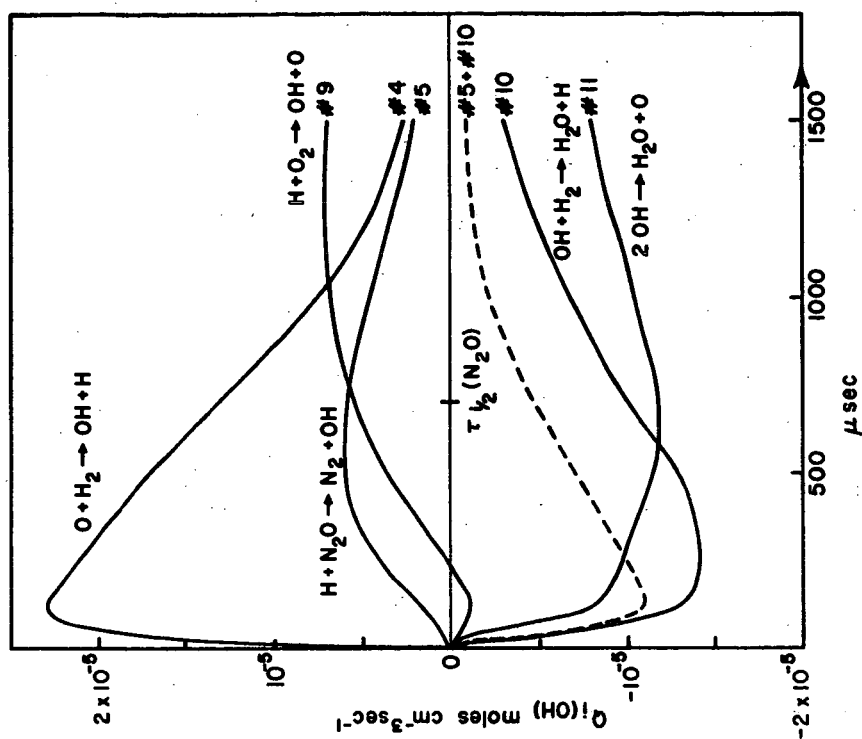
Figure 2a. Typical profiles for OH production rates from various reactions; 1st test on $N_2O/H_2 = 1:1$.
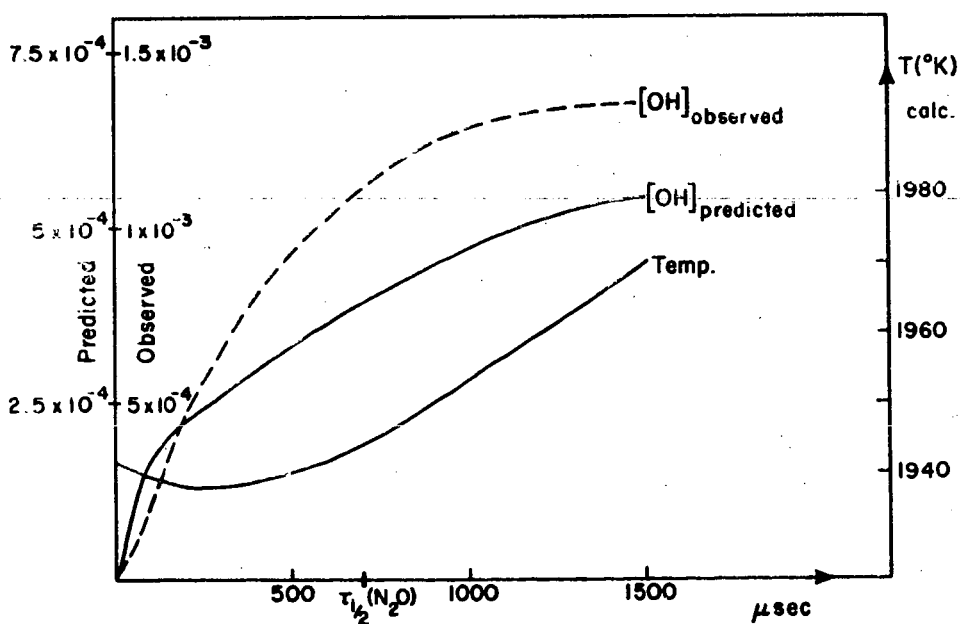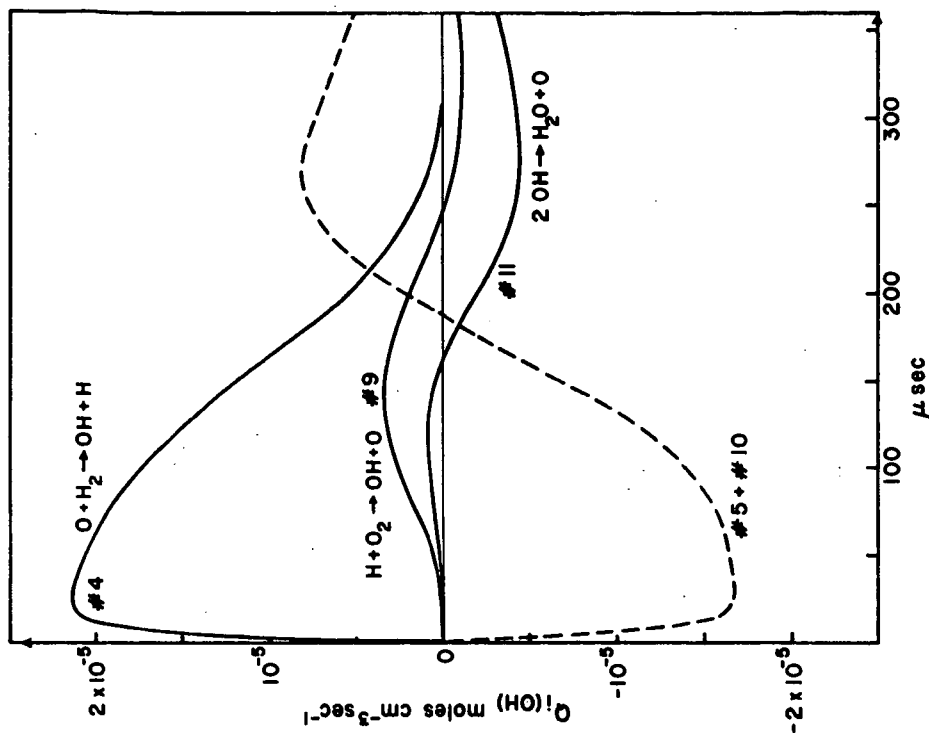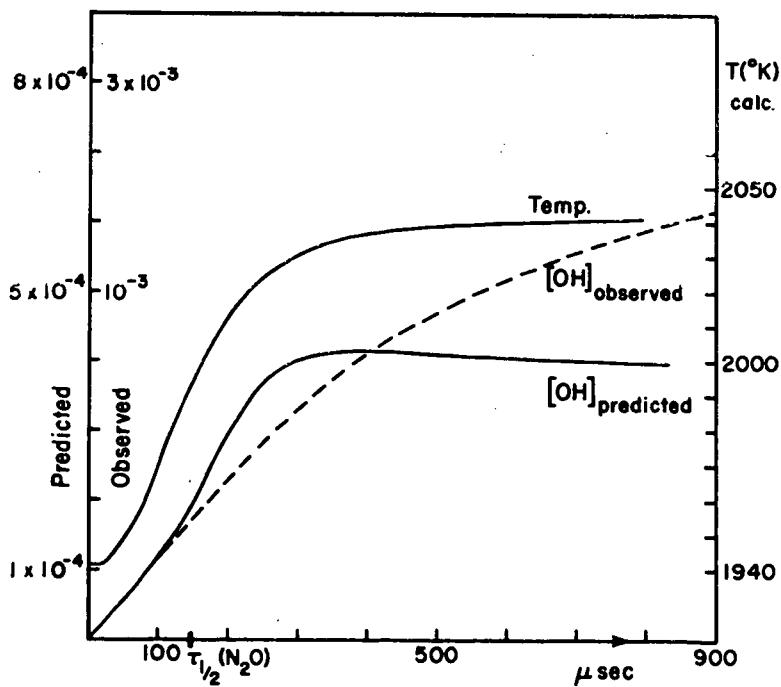

Figure 2b. Net [OH] produced, as a function of time.

Figure 3a. Second test; OH production rates for $N_2O/H_2 = 1:1$ (same as 2a).

Figure 3b. Net [OH] produced, as a function of time.